

## From lattice QCD to in-medium heavy-quark interactions via deep learning

Shuzhe Shi,<sup>a,\*</sup> Kai Zhou,<sup>b</sup> Jiaxing Zhao,<sup>c</sup> Swagato Mukherjee<sup>d</sup> and Pengfei Zhuang<sup>c</sup>

<sup>a</sup>Department of Physics, McGill University, Montreal, Quebec H3A 2T8, Canada.

<sup>b</sup>Frankfurt Institute for Advanced Studies, Ruth Moufang Strasse 1, D-60438, Frankfurt am Main, Germany.

<sup>c</sup>Department of Physics, Tsinghua University, Beijing 100084, China.

<sup>d</sup>Physics Department, Brookhaven National Laboratory, Upton, New York 11973, USA.

E-mail: [shuzhe.shi@mcgill.ca](mailto:shuzhe.shi@mcgill.ca)

Bottomonium states are key probes for studies of the quark-gluon plasma (QGP) created in high-energy nuclear collisions. Theoretical models of bottomonium productions in high-energy nuclear collisions rely on the in-medium interactions between the bottom and antibottom quarks, which can be characterized by real ( $V_R(T, r)$ ) and imaginary ( $V_I(T, r)$ ) potentials, as functions of temperature and spatial separation. Recently, the masses and thermal widths of up to  $3S$  and  $2P$  bottomonium states in QGP were calculated using lattice quantum chromodynamics (LQCD). Starting from these LQCD results and through a novel application of deep neural network, here, we obtain results for  $V_R(T, r)$  and  $V_I(T, r)$ . The temperature dependence of  $V_R(T, r)$  was found to be very mild between  $T \approx 0 - 330$  MeV. Meanwhile,  $V_I(T, r)$  shows a rapid increase with  $T$  and  $r$ , which is much larger than the perturbation theory-based expectations.

*The 38th International Symposium on Lattice Field Theory, LATTICE2021 26th-30th July, 2021  
Zoom/Gather@Massachusetts Institute of Technology*

---

\*Speaker

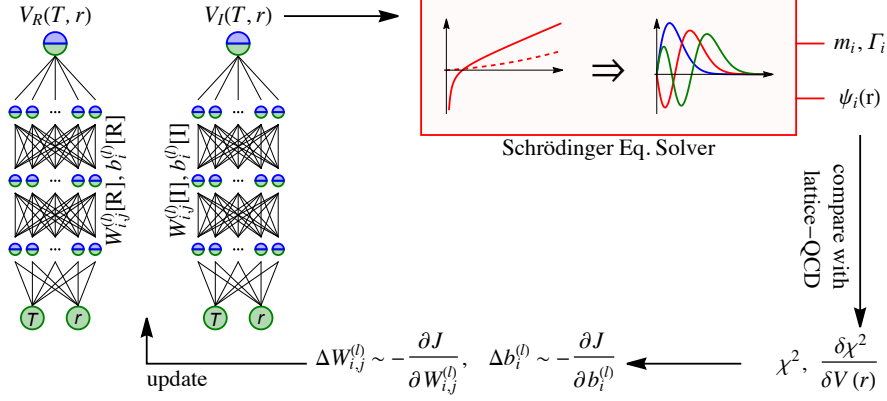


**Figure 1:** Flow chart of the potential reconstruction scheme — using generalized back-propagation to optimize parameters in the deep neural networks coupled with a Schrödinger equation.

## 1. Introduction

In-medium modifications of quarkonium states are sensitive probes of the QGP produced in high energy nuclear collisions [1, 2]. Sequential suppression patterns among the  $\Upsilon(1S)$ ,  $\Upsilon(2S)$  and  $\Upsilon(3S)$  states have been observed in heavy-ion collision experiments [3–6]. These experimental observations are understood in effective field theories (EFT), which naturally lead to an open quantum system based treatment of both open and hidden bottom states in QGP (see [7] for a recent review). If interactions between the color-singlet and color-octet states are neglected then the pNRQCD reduces to a theoretical description of quarkonia solely based on a potential between the heavy quark and antiquark. A potential based description allows studies of quarkonia by employing Schrödinger-type equations [8–11]. One-loop hard thermal loop (HTL) perturbative QCD calculations [12, 13], and later on pNRQCD calculations [14, 15], show that at finite temperatures heavy quark potential becomes complex with a nonvanishing imaginary part. However, it is difficult to provide satisfactory descriptions of bound states arising out of strong interactions solely using perturbative expansions and a nonperturbative treatment, such as the LQCD, is called for. In the static limit, the heavy quark potential can be extracted from the spectral functions of the thermal Wilson loop using nonperturbative LQCD calculations [16–19]. On the other hand, recent LQCD studies have led to quantification of the masses, thermal widths, and Bethe–Salpeter amplitudes (BSA) of up to  $3S$  and  $2P$  bottomonium states in QGP [20–22]. As we shall see later, one-loop HTL motivated functional forms of  $V_R(T, r)$  and  $V_I(T, r)$  are not compatible with the recent LQCD results. This observation calls for a model-independent nonperturbative extraction of the in-medium heavy quark potential.

In our recent work [23], we have developed a model-independent DNN-based method and determine the  $r$  and  $T$ -dependence of the in-medium heavy quark potential starting from the LQCD results [21] for the masses and thermal widths of up to  $3S$  and  $2P$  bottomonium states at various temperatures. The underlying idea is as follows: At a fixed  $T$ , various bottomonium states differ in sizes and their wavefunctions concentrate on different distances. Knowledge of the masses and thermal widths of multiple bottomonium states, thereby, provide constraints on not only the

strength of the real and imaginary parts of the bottom-antibottom interactions in QGP but also its  $r$ -dependence. Thus, LQCD results for the masses and thermal widths of multiple bottomonium states at different temperature can be used to extract  $V_R(T, r)$  and  $V_I(T, r)$  and, presently, DNN is probably the best tool achieve this in an unbiased fashion. According to the universal approximation theorem [24, 25], DNN can generally provide an unbiased, yet flexible enough, parameterization to approximate arbitrary functional relations. We exploited the DNNs to represent the real and imaginary potentials,

$$V_R(T, r) = V_{R, \text{DNN}}(\mathbf{b}_R, \mathbf{W}_R; T, r), \quad V_I(T, r) = V_{I, \text{DNN}}(\mathbf{b}_I, \mathbf{W}_I; T, r), \quad (1)$$

where  $\mathbf{b}$  and  $\mathbf{W}$  — called *bias* and *weight*, respectively — are the DNN parameters to be determined by fitting the LQCD masses and thermal widths [21].

## 2. Methodology

In typical machine-learning problems, one usually knows some direct informations of the target function — *e.g.*, its value at discrete points — and is able to tune the DNN parameters by directly compare its output to the known knowledge. In our network, however, we cannot compare Eq. (1) to the LQCD masses and thermal widths and fix the parameters. There is an extra step to map the DNN output (potential) to observables (masses and thermal widths) — the reduced complex-valued two-body time-independent Schrödinger equation,<sup>1</sup>

$$-\frac{\nabla^2}{m_b} \psi_n + [V_R(T, r) + i \cdot V_I(T, r)] \psi_n = E_n \psi_n, \quad (2)$$

where the wavefunction  $\psi_n$  and the energy eigenvalues  $E_n$  for in-medium bottomonia are complex-valued. Here,  $V_I(T=0, r) = 0$ ,  $\text{Re}[E_n] = m_n - 2m_b$  and  $\text{Im}[E_n] = -\Gamma_n$ , where  $m_n$  and  $\Gamma_n$  are the mass and thermal width of the  $n^{\text{th}}$  bottomonium state, respectively. We solved Eq. (2) with potential provided by DNN (1) and obtain the masses and thermal widths. The DNN parameters ( $b_i^{(l)}$  and  $W_{ij}^{(l)}$ ) are tuned by minimizing the cost function

$$J = \frac{\lambda}{2} \sum_{l,i} \left(b_i^{(l)}\right)^2 + \frac{\lambda}{2} \sum_{l,i,j} \left(W_{ij}^{(l)}\right)^2 + \frac{1}{2} \sum_{T,n} \left(\frac{m_{T,n} - m_{T,n}^{\text{LQCD}}}{\delta m_{T,n}^{\text{LQCD}}}\right)^2 + \left(\frac{\Gamma_{T,n} - \Gamma_{T,n}^{\text{LQCD}}}{\delta \Gamma_{T,n}^{\text{LQCD}}}\right)^2, \quad (3)$$

Here, the  $\propto \lambda$  terms are regularizers in DNN to avoid over-fitting. The summation runs over six temperature points,  $T \in \{0, 151, 173, 199, 251, 334\}$  MeV, and five bottomonium states,  $n \in \{1S, 2S, 3S, 1P, 2P\}$  and the LQCD values were taken from Ref. [21]. We used gradient descent with Back-Propagation optimization technique, which is based on the derivatives of the cost function with respect to the network parameters. We overcame the challenge of gradients evaluation of such implicit functions through perturbative solution of the Schrödinger equation with respect to small change of  $V(T, r)$ . Moreover, we invoked Bayesian inference for uncertainty quantification, whereby the posterior distribution of the network parameters was evaluated. In Fig. 1 we show the

<sup>1</sup>By taking the Cornell potential, we can well reproduce the vacuum masses of up to 3S and 2P bottomonium states [26] and the corresponding vacuum BSA obtained from LQCD calculation [22], (see [23] for more details).

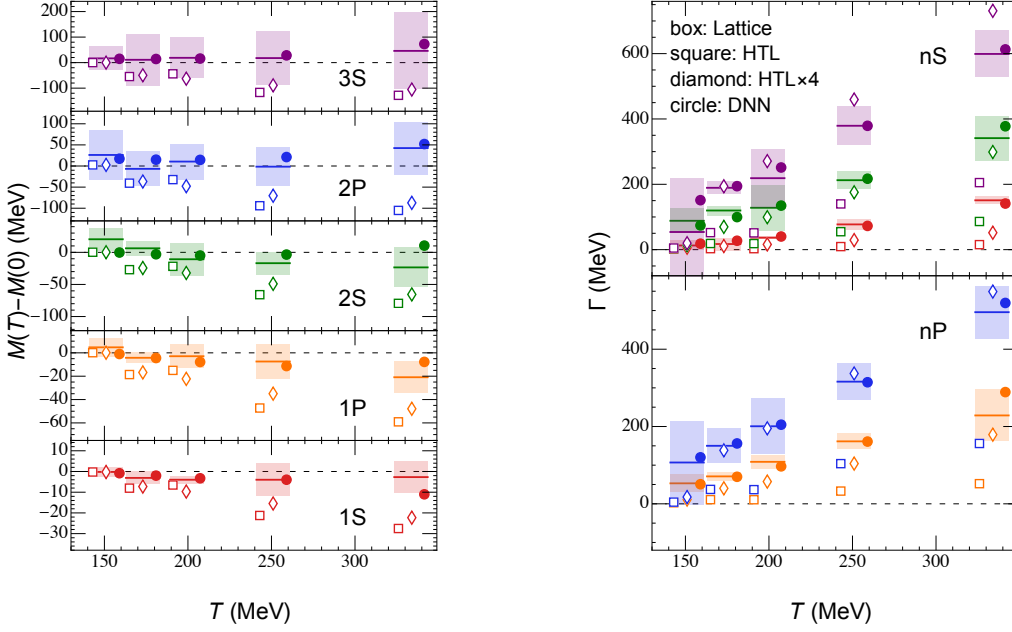


**Figure 2:** In-medium mass shifts (left) and the thermal widths (right) of different bottomonium states obtained from fits to LQCD results [21] (lines and shaded bands) using HTL functional forms [27] (open symbols) and DNN based optimization (filled circle). The points are shifted horizontally for better visualization.  $\Upsilon(1S)$ ,  $\chi_{b_0}(1P)$ ,  $\Upsilon(2S)$ ,  $\chi_{b_0}(2P)$  and  $\Upsilon(3S)$  states are represented by red, orange, green, blue, and purple symbols, respectively.

flow chart of our methodology of the potential reconstruction with DNNs coupled to a Schrödinger equation. To the best of our knowledge, the current method is developed for the first time here. More details on the method is provided in [23], along with a closure test to justify our methodology and assess its reliability.

### 3. Results

We begin with pointing out the inadequacy of weak-coupling motivated functional form of the potential to consistently describe the LQCD masses and thermal widths. We chose the functional form proposed in Ref. [27], which incorporates one-loop HTL based functional forms of  $V_I$  and of color-electric screening, in addition to a vacuum potential satisfying Gauss's law. Taking this functional form for the potential, we fix  $\alpha$ ,  $\sigma$ , and  $B$  by their vacuum values, and tune  $\mu_D$  at different temperatures to fit the finite-temperature bottomonia masses and widths. As shown by the open squares in Fig. 2, one-loop HTL motivated functional form of  $V_I$  and color-electric screening in  $V_R$  fail to simultaneously reproduce the LQCD results for the mass shifts and the thermal widths of bottomonium. Even if allowing an extra magnification factor for  $V_I$ , one would still miss the state-dependence of the thermal width (see open diamonds which take magnification factor to be four). The failure of the only known analytic form to describe the LQCD results necessitates a model-independent extraction of  $V(T, r)$  using an adequate unbiased parameterization. We devised the above outlined method by coupling Schrödinger equation with DNNs and achieved good agreement

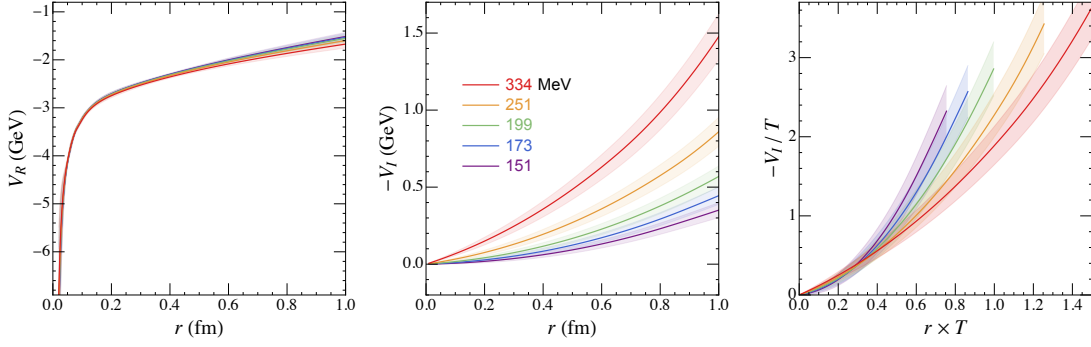


**Figure 3:** The DNN reconstructed real (Left) and imaginary (Middle) parts of the heavy quark potential at temperatures  $T = 151$ (purple),  $173$ (blue),  $199$ (green),  $251$ (orange), and  $334$  MeV(red). The uncertainty bands represent the  $68\%(1\sigma)$  confident region. Right panel is the same as Middle, but for  $x$ - and  $y$ -axis scaled by temperature  $T$ .

with the LQCD results [21] (see solid symbols in Fig. 2).

The  $T$ - and  $r$ -dependence of the extracted real and imaginary potentials are shown in Fig. 3. We see signs that with increasing temperature  $V_R(T, r)$  becomes flatter at large  $r$ , as expected from color screening effect. However, the temperature dependence of  $V_R(T, r)$  is very mild between  $T \approx 150 - 330$  MeV, and closely approximating its vacuum counterpart. In the same temperature range, we observed that  $V_I(T, r)$  monotonically increases both with temperature and distance. Whereas  $V_I$  varies a lot as temperature changes, the scaled imaginary potential,  $V_I/T$  as function of  $r \times T$ , is insensitive to the change of temperature, (see Right panel of Fig. 3).

The heavy quark potential obtained here is based on LQCD calculations of bottomonium state using 2+1 flavor dynamical gauge field background with nearly physical values of up, down, and strange quark masses. Our results for the heavy quark potential is qualitatively different from the static quark potentials extracted from the thermal spectral functions [16–19]. Unlike the previous studies, the  $V_R$  obtained in this work show very little signs of color-electric Debye screening for  $r \lesssim 1$  fm for the entire temperature range  $T \in [0, 334]$  MeV. The  $V_I$  here is much larger in magnitude and increases more rapidly both with  $T$  and  $r$  than the one-loop HTL motivated extractions. On the other hand, it is reassuring that the preliminary results on the static quark potential from very recent LQCD calculations and without using the one-loop HTL motivated forms are quite similar to the potential obtained here [28].

Finally, we compare the finite temperature wave-functions with the corresponding Bethe–Salpeter(BS) amplitudes from the lattice QCD calculation [22], which is obtained consistently with the masses and widths [21]. With such complementary information, the comparison serve as an independent test of the finite temperature potential. In Fig. 4 (Left), we compare the real part of wave-functions at different temperatures and observe mild temperature dependence of the BS amplitudes, while the wave-functions are obviously different at higher temperature. As noted in Ref. [22], due their non-trivial Euclidean-time dependence, the BSAs at  $T > 0$  fail to capture the thermal broadening of the states, rather resemble the vacuum wave-functions. Consequently, we

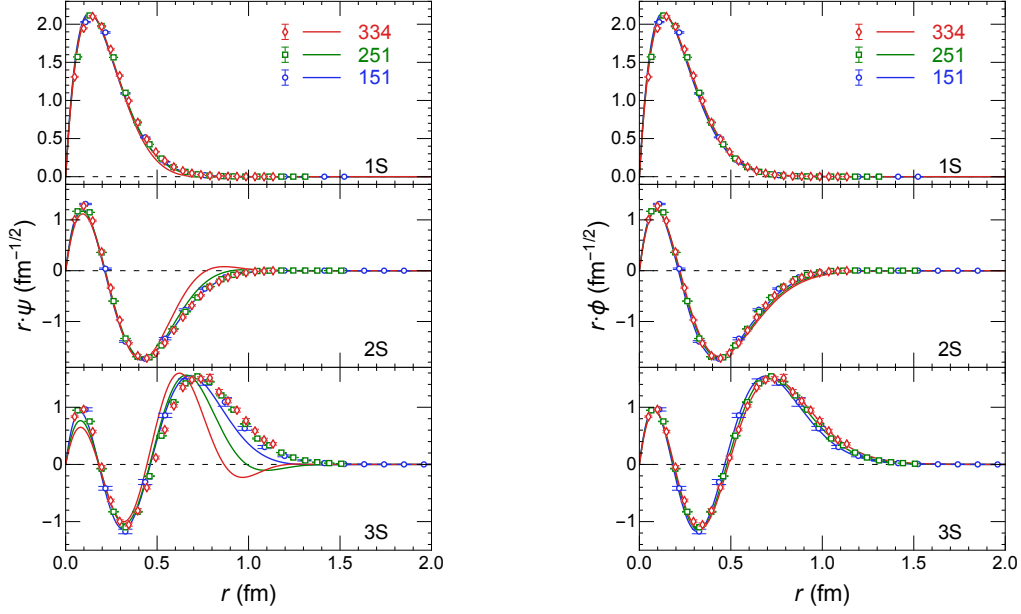


**Figure 4:** (left) Comparison of the real part of finite temperature wave-functions (curves) and Bethe–Salpeter amplitudes (symbol). Results at  $T=151, 251,$  and  $334$  MeV are respectively colored in blue, green, and red. (Right) Same as Left but for “pseudo-wave-function” obtained only from the real potential. See text for explanation.

solve the “pseudo-wave-functions”, denoted as  $\phi$ , according to the real potential in Fig. 3,

$$-\frac{\nabla^2}{m_b} \phi_n + V_R(T, r) \phi_n = \tilde{E}_n \phi_n, \quad (4)$$

and compare them with the BS amplitude in Fig. 4 (Right), and find excellent agreement especially regarding the large- $r$  tail at different temperatures. Such comparison independently verifies the real part of the interaction potential at finite temperature. In particular, the tail behavior of the wave-functions is sensitive to the flatness of the potential at  $r \gtrsim 0.5$  fm. The excellent agreement shown in Fig. 4 (Right), especially for the 3S state at all temperatures, confirms the weak screening effect observed in the real part of the potential.

#### 4. Conclusion

In this work, the in-medium heavy quark potential with a bias-free DNN representation is determined from the recently obtained LQCD results [21] for the masses and thermal widths of up to 3S and 2P bottomonium states in QGP. By coupling the Schrödinger equation to the DNN, we introduced a novel method for unbiased extractions of the real and imaginary parts of the heavy quark potential, and invoked Bayesian inference to quantify the potential uncertainties in a non-local fashion. We obtained  $V_R(T, r)$  and  $V_I(T, r)$  for  $r \lesssim 1$  fm and  $T \lesssim 330$  MeV. The  $V_R(T, r)$  has very mild  $T$  dependence and closely resembles the vacuum potential. On the other hand,  $V_I(T, r)$  is large and rises rapidly with  $T$  and  $r$ . These results are qualitatively different from the static quark

potential obtained using one-loop HTL perturbative calculations. It would be very interesting to see the phenomenological consequences of this heavy quark potential, model-independently extracted from the non-perturbative LQCD calculations.

We end by discussing the possible model-dependence of our results. As far as we can tell, there is no bias or model-dependence in the potential extraction method, thus the only possible dependence comes from the prior used in the LQCD calculation of masses and thermal widths, which is not possible to avoid. We look forward to perform our potential extraction method to more upcoming available LQCD results of masses and thermal widths for ground states and excitations.

*Acknowledgement* — This material is based upon work supported by: (i) The NSFC under grant Nos. 11890712 and 12075129 and Guangdong Major Project of Basic and Applied Basic Research No. 2020B0301030008 (J.Z. and P.Z.); (ii) The Natural Sciences and Engineering Research Council of Canada (S.S.); (iii) The Fonds de recherche du Québec - Nature et technologies (FRQNT) through the Programme de Bourses d'Excellence pour Étudiants Étrangers (PBEEE) scholarship (S.S.); (iv) The BMBF funding under the ErUM-Data project and the AI grant at FIAS of SAMSON AG, Frankfurt (K.Z.); (v) The GPU Grant of the NVIDIA Corporation (K.Z.); (vi) The U.S. Department of Energy, Office of Science, Office of Nuclear Physics through the Contract No. DE-SC0012704 (S.M.); (vii) The U.S. Department of Energy, Office of Science, Office of Nuclear Physics and Office of Advanced Scientific Computing Research, within the framework of Scientific Discovery through Advance Computing (SciDAC) award Computing the Properties of Matter with Leadership Computing Resources (S.M.).

## References

- [1] T. Matsui and H. Satz, *J/ψ Suppression by Quark-Gluon Plasma Formation*, *Phys. Lett. B* **178** (1986) 416.
- [2] F. Karsch, M.T. Mehr and H. Satz, *Color Screening and Deconfinement for Bound States of Heavy Quarks*, *Z. Phys. C* **37** (1988) 617.
- [3] CMS collaboration, *Indications of suppression of excited Υ states in PbPb collisions at  $\sqrt{s_{NN}} = 2.76$  TeV*, *Phys. Rev. Lett.* **107** (2011) 052302 [1105.4894].
- [4] CMS collaboration, *Observation of Sequential Upsilon Suppression in PbPb Collisions*, *Phys. Rev. Lett.* **109** (2012) 222301 [1208.2826].
- [5] CMS collaboration, *Suppression of Υ(1S), Υ(2S) and Υ(3S) production in PbPb collisions at  $\sqrt{s_{NN}} = 2.76$  TeV*, *Phys. Lett. B* **770** (2017) 357 [1611.01510].
- [6] CMS collaboration, *Suppression of Excited Υ States Relative to the Ground State in Pb-Pb Collisions at  $\sqrt{s_{NN}}=5.02$  TeV*, *Phys. Rev. Lett.* **120** (2018) 142301 [1706.05984].
- [7] X. Yao, W. Ke, Y. Xu, S.A. Bass and B. Müller, *Coupled Boltzmann Transport Equations of Heavy Quarks and Quarkonia in Quark-Gluon Plasma*, *JHEP* **21** (2020) 046 [2004.06746].
- [8] H. Satz, *Colour deconfinement and quarkonium binding*, *J. Phys. G* **32** (2006) R25 [hep-ph/0512217].

- [9] J. Zhao, K. Zhou, S. Chen and P. Zhuang, *Heavy flavors under extreme conditions in high energy nuclear collisions*, *Prog. Part. Nucl. Phys.* **114** (2020) 103801 [2005.08277].
- [10] H.W. Crater, J.-H. Yoon and C.-Y. Wong, *Singularity Structures in Coulomb-Type Potentials in Two Body Dirac Equations of Constraint Dynamics*, *Phys. Rev. D* **79** (2009) 034011 [0811.0732].
- [11] X. Guo, S. Shi and P. Zhuang, *Relativistic Correction to Charmonium Dissociation Temperature*, *Phys. Lett. B* **718** (2012) 143 [1209.5873].
- [12] M. Laine, O. Philipsen, P. Romatschke and M. Tassler, *Real-time static potential in hot QCD*, *JHEP* **03** (2007) 054 [hep-ph/0611300].
- [13] A. Beraudo, J.P. Blaizot and C. Ratti, *Real and imaginary-time  $Q$  anti- $Q$  correlators in a thermal medium*, *Nucl. Phys. A* **806** (2008) 312 [0712.4394].
- [14] N. Brambilla, J. Ghiglieri, A. Vairo and P. Petreczky, *Static quark-antiquark pairs at finite temperature*, *Phys. Rev. D* **78** (2008) 014017 [0804.0993].
- [15] N. Brambilla, M.A. Escobedo, J. Ghiglieri, J. Soto and A. Vairo, *Heavy Quarkonium in a weakly-coupled quark-gluon plasma below the melting temperature*, *JHEP* **09** (2010) 038 [1007.4156].
- [16] A. Rothkopf, T. Hatsuda and S. Sasaki, *Complex Heavy-Quark Potential at Finite Temperature from Lattice QCD*, *Phys. Rev. Lett.* **108** (2012) 162001 [1108.1579].
- [17] Y. Burnier, O. Kaczmarek and A. Rothkopf, *Static quark-antiquark potential in the quark-gluon plasma from lattice QCD*, *Phys. Rev. Lett.* **114** (2015) 082001 [1410.2546].
- [18] Y. Burnier, O. Kaczmarek and A. Rothkopf, *Quarkonium at finite temperature: Towards realistic phenomenology from first principles*, *JHEP* **12** (2015) 101 [1509.07366].
- [19] D. Bala and S. Datta, *Nonperturbative potential for the study of quarkonia in QGP*, *Phys. Rev. D* **101** (2020) 034507 [1909.10548].
- [20] R. Larsen, S. Meinel, S. Mukherjee and P. Petreczky, *Thermal broadening of bottomonia: Lattice nonrelativistic QCD with extended operators*, *Phys. Rev. D* **100** (2019) 074506 [1908.08437].
- [21] R. Larsen, S. Meinel, S. Mukherjee and P. Petreczky, *Excited bottomonia in quark-gluon plasma from lattice QCD*, *Phys. Lett. B* **800** (2020) 135119 [1910.07374].
- [22] R. Larsen, S. Meinel, S. Mukherjee and P. Petreczky, *Bethe-Salpeter amplitudes of Upsilon's*, *Phys. Rev. D* **102** (2020) 114508 [2008.00100].
- [23] S. Shi, K. Zhou, J. Zhao, S. Mukherjee and P. Zhuang, *Heavy Quark Potential in QGP: DNN meets LQCD*, **2105.07862**.

- [24] M. Leshno and S. Schocken, *Multilayer feedforward networks with a nonpolynomial activation function can approximate any function*, *Neural Networks* **6** (1993) 861.
- [25] A. Kratsios, *The universal approximation property*, *Annals of Mathematics and Artificial Intelligence* (2021) .
- [26] PARTICLE DATA GROUP collaboration, *Review of Particle Physics*, *Phys. Rev. D* **98** (2018) 030001.
- [27] D. Lafferty and A. Rothkopf, *Improved Gauss law model and in-medium heavy quarkonium at finite density and velocity*, *Phys. Rev. D* **101** (2020) 056010 [1906.00035].
- [28] D. Bala, O. Kaczmarek, R. Larsen, S. Mukherjee, G. Parkar, P. Petreczky et al., *Static quark anti-quark interactions at non-zero temperature from lattice QCD*, 2110.11659.